JOURNAL OF MATERIALS SCIENCE 32 (1997) 1461–1467

Synthesis and structural evolution of tungsten carbide prepared by ball milling

G. M. WANG, S. J. CAMPBELL
School of Physics, University College, University of New South Wales, Australian Defence Force Academy, Canberra, ACT 2600, Australia

A. CALKA
Department of Materials Engineering, University of Wollongong, Wollongong, New South Wales 2522, Australia

W. A. KACZMAREK
Department of Applied Mathematics, RSPhysSE, The Australian National University, Canberra, ACT0200, Australia

Tungsten carbide has been synthesized directly by ball-milling tungsten powder and activated carbon in vacuum. The structural development of the WC phase with milling times up to 310 h has been followed using X-ray, neutron diffraction and scanning electron microscopy. Subsequent annealing (at 1000 °C for 1 and 20 h) of material milled for 90 h or longer, results in samples comprising almost entirely crystalline WC. The production of WC itself during milling results in enhanced iron contamination from the steel mill and balls on extended milling which were monitored by energy-dispersive X-ray and Mössbauer spectroscopies.

1. Introduction

The outstanding hardness properties of tungsten carbide are well known and, as such, WC has been used extensively in industry, particularly the tool-cutting industry. Tungsten carbide is usually synthesized by direct reaction between tungsten and carbon at very high temperatures, typically 1400–1600 °C [1] under good vacuum or highly purified gas conditions. Recently, ball-milling and related methods of mechanochemical synthesis are proving important developments in the preparation of new phases and materials [2]. Although mechanosynthesis has been applied readily in the preparation of carbides and nitrides [3, 4], relatively little work has so far been carried out on the W–C system. Matteazzi and Le Caër [5] have recently reported the effects of milling a 50:50 atomic mixture of tungsten and carbon powders but because of contamination from their vial and balls (which were themselves made from tungsten carbide), they were unable to ascertain other than at most a partial carburization of tungsten in their vibratory ball mill.

Here we present the results of our investigation into the effects of milling tungsten and activated carbon powders using hardened stainless steel balls and a planar ball mill (Uni-Ball Mill [6]) which enables a range of energy conditions to be selected. The direct formation of tungsten carbide by mechanosynthesis has been confirmed by X-ray and neutron diffraction. The influence of milling conditions and particle morphology (as well as related heat treatments on the milled materials) on the formation of WC and W_2C has been investigated by X-ray diffraction (XRD) and scanning electron microscopy (SEM). Mössbauer effect spectroscopy has been useful in tracking the iron contamination which accrues with extended milling.

2. Experimental procedure

The milling was carried out under high-energy conditions using a specially designed ball-mill which allows magnetic control of the ball movement [6]. The starting materials were a 50:50 atomic mixture of tungsten powder (purity 99%, mean particle size $\sim 5\ \mu m$) and activated granular carbon (particle size $\sim$ 0.9–1.7 mm). Each 8 g charge of mixed powder was milled for periods of 45, 90, 170 and 310 h in vacuum ($\sim 10^{-2}$ Pa) using four hardened stainless steel balls. The ball to powder ratio was about 30:1. The structural developments taking place during milling and subsequent annealing were monitored using a Phillips X-ray diffractometer (XRD) with CoK_α radiation. The particle-size morphology and material composition were examined using a Cambridge scanning electron microscope equipped with an energy-dispersive X-ray (EDX) analyser. The anticipated presence of iron contamination on extended milling was checked by carrying out room-temperature ^{57}Fe Mössbauer spectroscopy on the milled and subsequently annealed samples using a standard spectrometer and ^{57}CoRh source. The spectrometer was calibrated using a standard α-Fe foil and the spectra are presented relative to

0022–2461 © *1997 Chapman & Hall*

the centre of an α-Fe spectrum. Complementary differential thermal analysis measurements were carried out using a Shimadzu DTA-50 analyser with samples heated at a rate of about 20 °C min^{-1} in argon.

3. Results and discussion

3.1. Formation of tungsten carbides by milling

The X-ray diffraction (XRD) patterns of the starting W50–C50 mixture and the as-milled material at the different milling times are shown in Fig. 1. The structural changes caused by milling can be concluded as follows. First, the tungsten diffraction peaks remain as the dominant features for samples milled for 45 and 90 h but evidence for the formation of the WC phase is obtained in the materials milled for 170 h and, in more pronounced form, in the 310 h milled sample. Considering the mill and balls we used are made from stainless steel, there is no doubt that the WC phase presented in as-milled materials was produced by direct milling. Second, no intermediate phase was found according to Fig. 1, indicating WC phase was synthesized directly on the basis of tungsten and carbon element powders. Third, an increased peak width of tungsten diffraction with increasing milling time for 45, 90 and 170 h was observed, reflecting the decrease in grain size or increase in strain of tungsten with milling progress. Indeed, the grain size of tungsten was estimated, using the Scherrer formula, as ~ 33 nm after 45 h milling, decreasing to 24 and 13 nm after 90 and 170 h milling, respectively. At the same time, the strain was found, based on the XRD data analysis, to be 0.5% for the 45 h milled sample, increasing to 1.2% and 1.3% after 90 and 170 h milling, respectively. In addition to the peak broadening, the lattice parameter of cubic tungsten was found to be slightly increased after milling ($a = 0.3168, 0.3166$ and 0.3169 nm for 45, 90 and 170 h milled samples, respectively) compared with the published value (0.3165 nm [7]). These results show the crystalline structure of tungsten was slightly distorted or a few carbon atoms have diffused into the tungsten lattice except the decrease in grain size during milling. No clear tungsten peaks but rather very broadened WC peaks were found after 310 h milling, demonstrating the nanocrystalline characteristic of the WC phase with a grain size of about 7 nm.

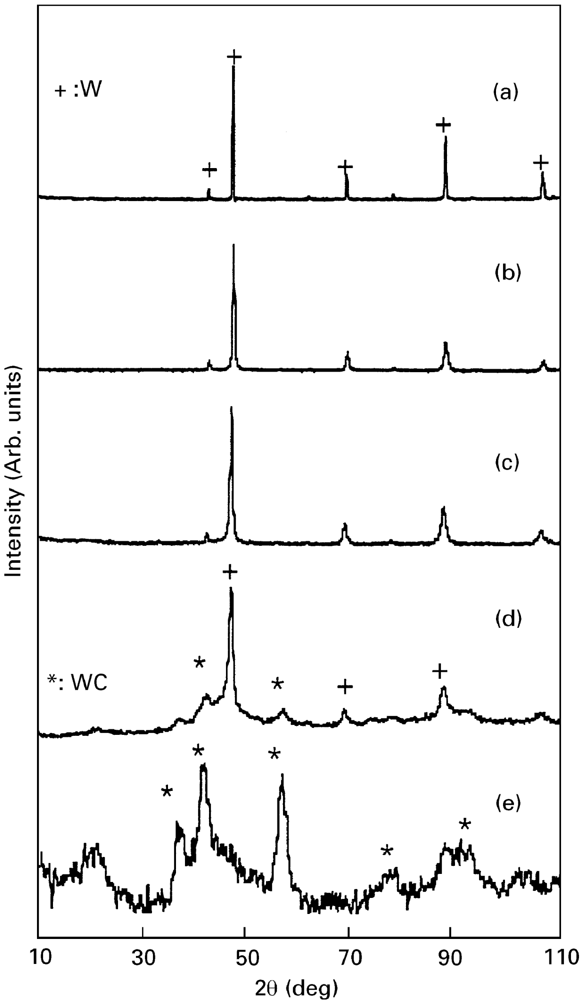

Figure 1 X-ray diffraction pattern of ball milled W50–C50 powders: (a) starting powder, (b) 45 h, (c) 90 h, (d) 170 h and (e) 310 h.

Because of the slightly poor signal to background ratio in Fig. 1e, we decided to check the structural feature of as-milled samples by running the neutron diffraction experiment. Two representative samples (45 and 310 h milled) were used to carry out this experiment (see Fig. 2). About nine clear peaks were observed for 310 h milled samples (Fig. 2b). Seven of them, the predominant part of the diffraction, have *d* values of 0.25, 0.188, 0.145, 0.129, 0.123, 0.115 and 0.09 nm, which are exactly the *d* values of WC (0 0 1), (1 0 0), (1 1 0), (1 1 1), (1 0 2), (2 0 1) and (2 1 1) diffraction planes [8]. Another two peaks with *d* values of 0.206 and 0.174 nm do not belong to WC, but match W_2C (1 0 0) and (1 0 2) diffractions. In addition to the carbides, there is also possibly a trace of tungsten which overlaps the WC diffraction. While the peaks found in the diffraction pattern of 45 h milled samples (Fig. 2a) with *d* values of 0.224, 0.158, 0.130, 0.113, 0.102 and

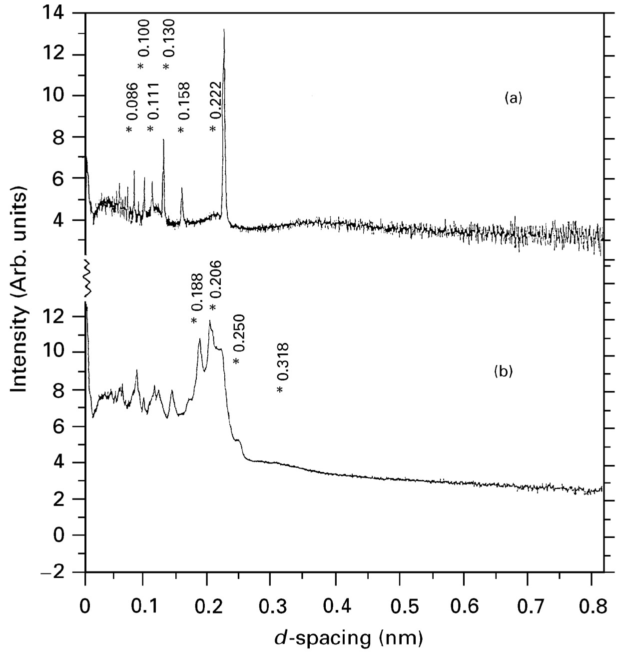

Figure 2 Neutron diffraction patterns of samples milled for (a) 45 h and (b) 310 h.

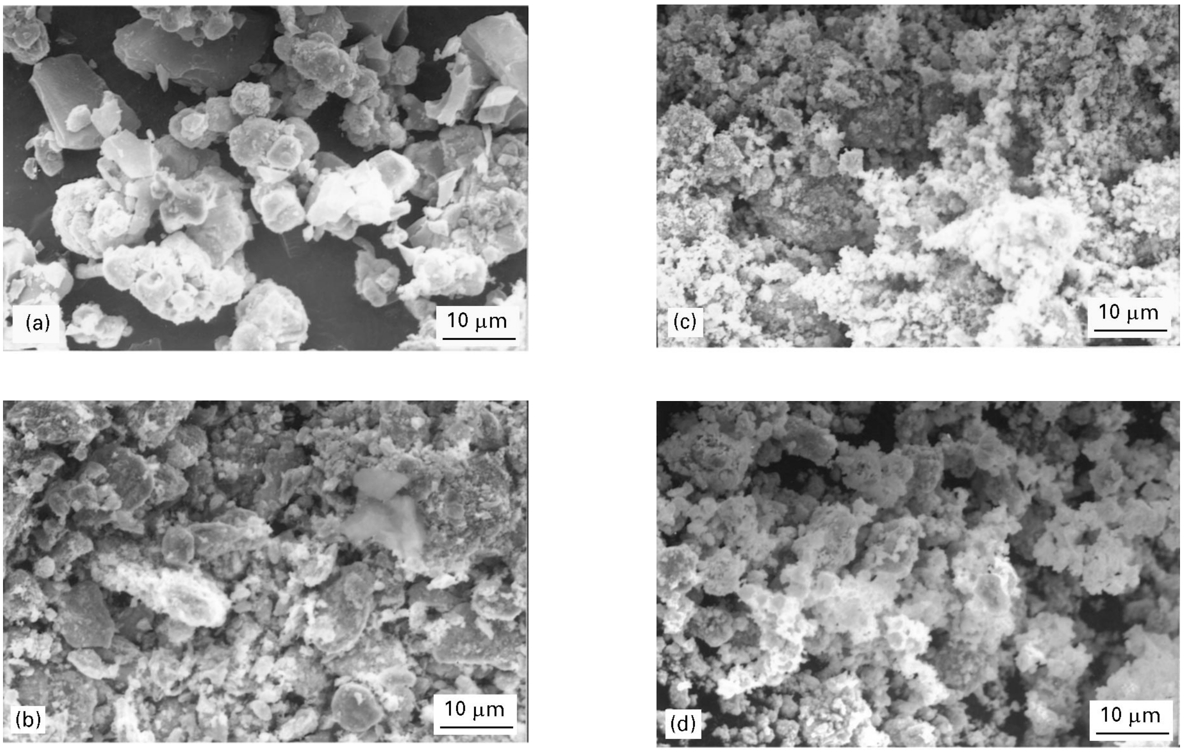

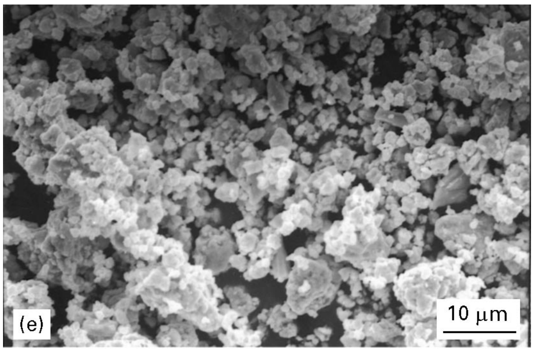

Figure 3 SEM images of ball milled W50–C50 powders: (a) starting powder, (b) 45 h, (c) 90 h, (d) 170 h and (e) 310 h.

0.085 nm agree very well with the tungsten (1 1 0), (2 0 0), (2 1 1), (2 2 0), (3 1 0) and (3 2 1) diffractions [7], no trace of carbides was found in the 45 h milled sample. By the above procedure, it is confidently confirmed that we have successfully produced WC alloy by direct milling of tungsten and activated carbon powders in vacuum under our experimental setting. In addition, it is also revealed that there is a small fraction of W_2C phase present in the as-milled materials, and also the starting tungsten has not been totally converted into tungsten carbides by milling for up to 310 h.

Differing from the X-ray diffraction analysis (Fig. 1), neutron diffraction also gives clear evidence of the presence of W_2C in the 310 h milled sample. This result is consistent with the phase diagram [9]. But it also raises the question: what is the relation between WC and W_2C phases during milling? In other words, is the conclusion that WC phase is formed based directly on the elements powder, correct? This question will be answered later in terms of thermal treatments.

As shown in Fig. 3, the SEM images indicate the morphological evolution after different milling times. There is a slight reduction in the average particle size of the material milled for 45 h compared with the starting material. Significant decreases in particle sizes to $\leqslant 1$ μm are, however, obtained in the materials milled for 90, 170 and 310 h. Similarly, the morphology of the particles remains relatively unchanged for the powders milled for 90, 170 and 310 h. The decreased tendency to nanoscale grain sizes estimated from the widths of the XRD peaks (see Fig. 1) compared with the particle size of $\leqslant 1$ μm and the unchanged morphology after 90, 170 and 310 h milling obtained from Fig. 2, indicate that the particles shown in Fig. 2 have a more and more complex substructure comprising these nanoscale grains with milling progress, which could reflect the structural transition from tungsten and carbon elements to WC alloy. Another significant difference, however, was the increased fraction of contaminant iron obtained with increasing milling time. A semi-quantitative analysis using EDX analysis showed a monotonic increase in the percentage of iron contamination present with milling time (Fig. 4). This will surely raise the question : why is there no iron trace in the XRD patterns (Fig. 1) while the EDX shows such a heavy iron contamination? There are three possible reasons for this. First, the EDX analyser does not sense light elements such as carbon; the amount of iron contamination, was thus measured related to the tungsten. In other words, above percentages of iron contamination are just a relative value to tungsten. The absolute values could be half of the above percentage, considering the different sensitive factors of the EDX detector to tungsten and iron. Second, the iron could be present in different forms or in distorted structures, say γ-austenite, W–Fe–C solid solutions and so on, which in all will broaden the diffraction

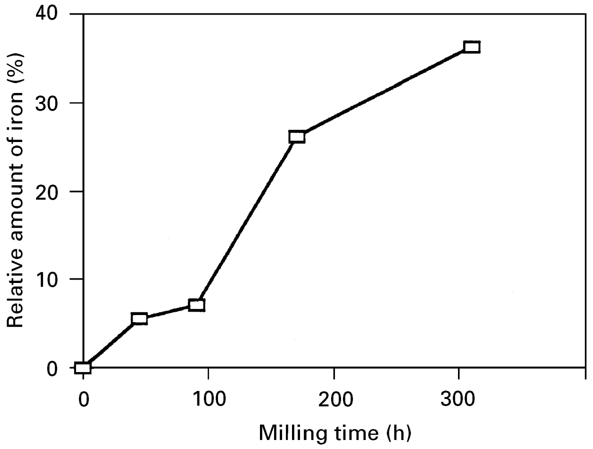

Figure 4 Relative contamination of iron as a function of milling time.

peak and reduce the intensity of the diffraction. The third reason is that the atomic scattering factor of iron to X-ray is far weaker than tungsten [10]. As a combined result, the intensity of tungsten in the XRD pattern is so strong that the diffraction from the small amount of iron was regarded as the same as the background. A similar effect was also observed in ball milling W34–Fe33–C33 [11]; virtually no iron but strong tungsten reflections were found in the XRD pattern after 50 h milling despite the percentages of tungsten and iron being almost the same. Regardless of the absolute values of iron contamination, an important feature in Fig. 4 is the rapid increase after more than 90 h milling. This appears to be further indication of WC formation. Because WC is a much harder material than stainless steel, it will scratch out the iron from the inside wall of the mill and the surfaces of the balls during the milling process. For short-term milling (not more than 90 h), where there is no WC present in the powders, a correspondingly slight iron contamination was found.

Room-temperature Mössbauer spectra of the milled samples were taken as a further check on the level of iron contamination resulting from milling (Fig. 5). Consistent with the expectation of increased iron contamination with increasing milling time, the relative absorption was found to increase from ~0.003% after 45 h milling to ⩽ 4% after 310 h milling. No magnetic hyperfine splitting was found in any spectra of the as-milled powders. The poor absorptions in Mössbauer spectra of 45 and 90 h milled samples lead to a meaningless fitting, while the spectra of 170 and 310 h milled samples exhibit generally a broadened doublet with parameters of IS ~0.3 mm s^{-1} and QS ~0.4 mm s^{-1}. It should be noted that relaxation effects, similar to those observed in the milling of $BaFe_{12}O_{19}$ [12], may occur in Mössbauer studies of ultrafine particles. However, the absence of a strongly magnetic phase in the Fe–W–C system suggests that relaxation effects are unlikely to account for the present doublet-like spectrum. Indeed, the spectrum for the 310 h milled sample appears to be similar to the paramagnetic spectrum obtained by milling W–Fe–C mixtures [11] in which a W–Fe–C solid solution was found in as-milled materials, transferring to W_3Fe_3C or W_6Fe_6C after heat treatments, depending on milling time and carbon composition. Similarly, we believe that the contaminating iron which resulted from the milling process is likely to be present in the form of the Fe–W–C solid solution. This solid solution will be transferred to ternary phases after annealing at 1000 °C as shown elsewhere [11]. This kind of transformation was observed in the heat treatment later. In addition, the spectra of Fig. 5 also demonstrate clearly that the rate of production of the iron contamination increases significantly for milling times greater than about 90 h. This is in good agreement with the X-ray diffraction (Fig. 1) in which peaks due to the WC phase are evident in the sample milled for 170 h and the EDX analysis in which a higher level of iron contamination, due to increased wear on the steel balls and sides of the mill, were found in 170 and 310 h milled materials.

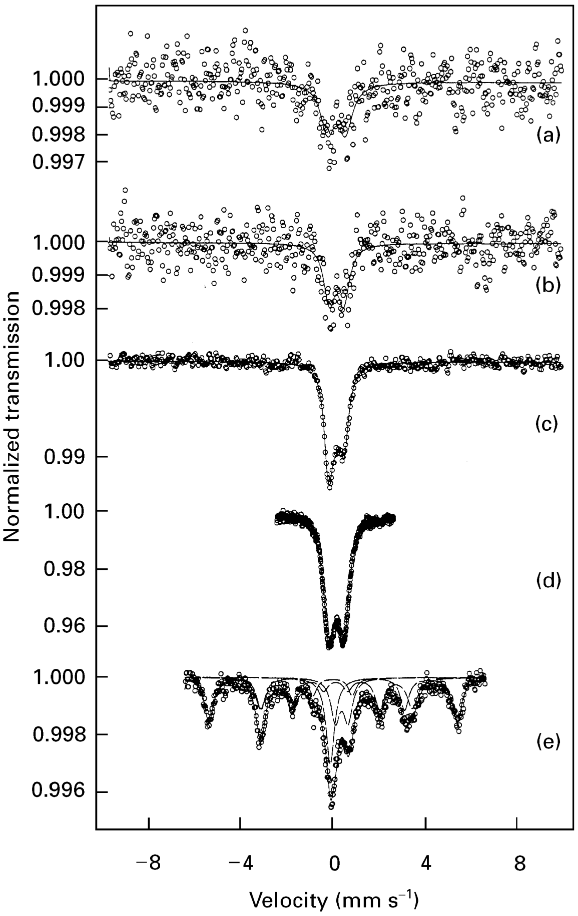

Figure 5 Room-temperature Mössbauer spectra of ball milled W50–C50 powders: (a) 45 h, (b) 90 h, (c) 170 h, (d) 310 h and (e) 310 h milled then 1000 °C/1 h annealed.

3.2. Effects of heat treatment

To investigate the thermal behaviour of these as-milled materials, differential thermal analysis (DTA) was carried out, which combined with the phase diagram [9] provides guidance to the heat treatment of the as-milled samples. Fig. 6 shows the DTA curves of the starting mixture and the as-milled powders. As can be seen, a clear exothermal peak around 900 °C appeared in the curve of the 45 h milled sample, slightly

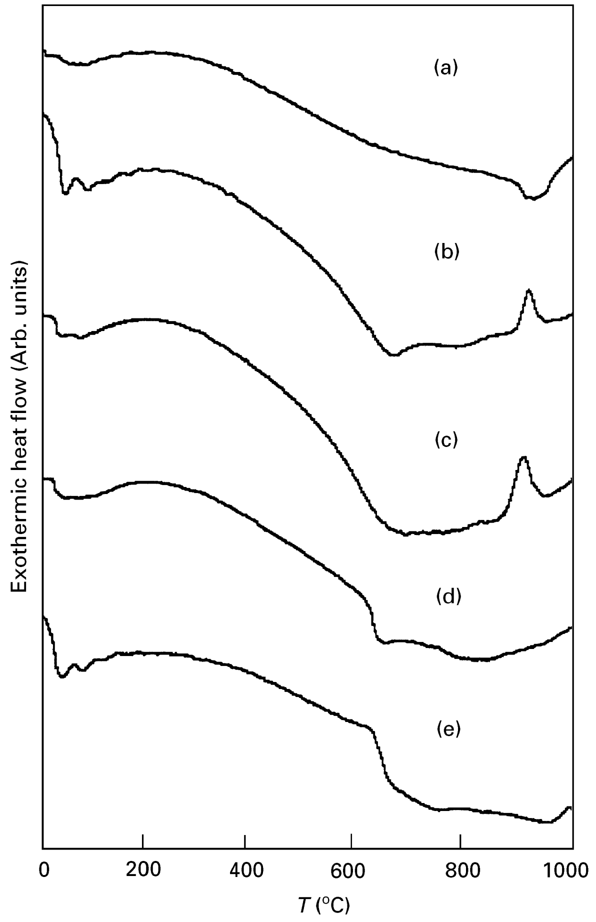

Figure 6 Differential thermal analysis of ball milled W50–C50 powders: (a) starting powder, (b) 45 h, (c) 90 h, (d) 170 h and (e) 310 h.

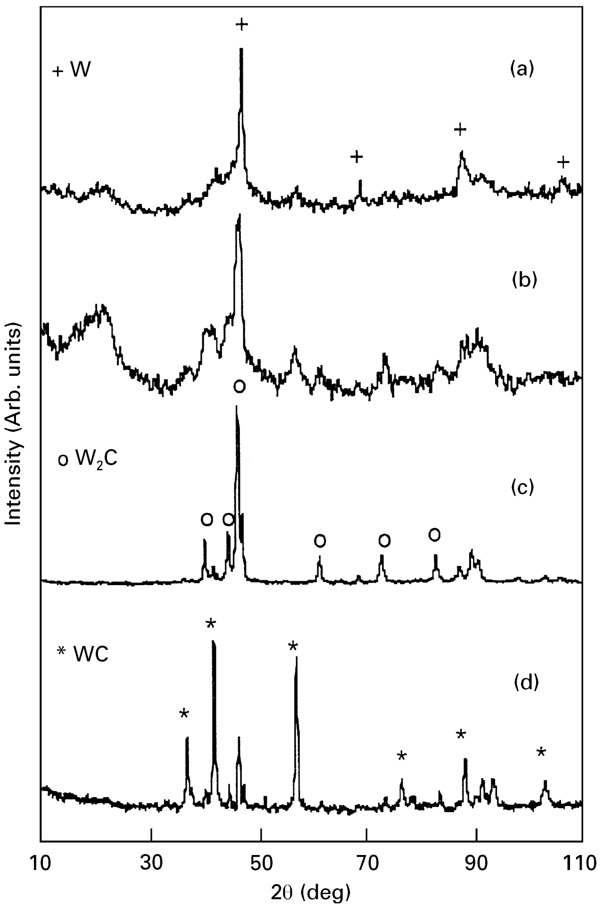

Figure 7 X-ray diffraction patterns of W50–C50 powder: (a) 170 h milled then 550 °C/10 min annealed, (b) 170 h milled then 700 °C/10 min annealed, (c) 90 h milled then 800 °C/10 min annealed, (d) 90 h milled and 900 °C annealed for 10 min.

increased in intensity after 90 h milling, and totally disappeared after 170 and 310 h milling. In addition, there is also a visible thermal flow change around 650 °C for all as-milled materials.

Accordingly, portions of the 90 h milled sample were annealed at 800 and 950 °C for 10 min in vacuum. The corresponding XRD patterns (Fig. 7c,d) show clearly W$_2$C phase after 800 °C annealing, but predominantly WC phase for 950 °C treatment. This allows us to conclude that the exothermic peak around 900 °C in the DTA curves represents the transformation of W$_2$C to WC phase. Similarly, annealings at 550 and 700 °C for 10 min were carried out using the 170 h milled material. No phase transition was found in this temperature range, according to XRD (Fig. 7a,b), except for the expected increased enhancement of WC structural features with increasing annealing temperature.

Based on above heat treatments, we can now fully understand the features of each DTA curve. Unreacted tungsten and activated carbon in the 45 and 90 h milled powders form W$_2$C when annealed at a temperature below 800 °C, which is consistent with the prediction of the phase diagram [9]. Annealing at a temperature over 900 °C results in the transformation of W$_2$C to WC phase although this should take place at a temperature over 2000 °C, according to the phase diagram [9]. Compared with the 45 h milled sample, the smaller particle size (see Fig. 3) in the 90 h milled powder facilitates the formation of W$_2$C and the transition of W$_2$C to WC. In other words, there is greater transition of W$_2$C to WC taking place in 90 h milled material than in the 45 h milled powder, which leads to the slightly increased intensity of the exothermic peak around 900 °C in the DTA curves. After more than 170 h milling, quite a lot of tungsten and carbon atoms have already formed primarily the structure of WC in the as-milled powders. Subsequent heat treatment results in the growth of WC without the formation of W$_2$C. As a consequence, the absence of the exothermic peak corresponded to the transition of W$_2$C to WC, was observed in their DTA curves.

As mentioned before, neutron and XRD measurements indicate there are no carbides in 45 h milled material. Considering this fact, the exothermic peak around 900 °C in the 45 h milled sample, corresponding to the transition of W$_2$C to WC phase, implies that the W$_2$C phase was formed by heat treatment, not by milling in this sample. A similar conclusion can be applied to the 90 h milled powder. In other words, there is basically no W$_2$C phase in the 45 and 90 h milled samples. After 170 and 310 h milling, we see a predominant trace of WC, a slight hint of W$_2$C phase, which suggests, on comparing with the 45 and 90 h milled samples, that WC was produced directly by milling based on the elemental powders, not based on the W$_2$C phase, otherwise W$_2$C phase would be observed in the as-milled materials first, then WC.

A small amount of W_2C phase and unreacted tungsten present in the 310 h milled sample as shown by neutron diffraction indicates the inhomogeneity of the milled sample and also shows that W_2C could be in the boundary regions in which less carbon is available.

The effects of annealing of the samples at 1000 °C in vacuum for 1 h are revealed by the series of XRD patterns in Fig. 8. This heat treatment produced a fraction of the W_2C phase and unreacted tungsten (and carbon) for the as-mixed powders, consistent with the phase diagram [9]. The ball milled samples exhibit different thermal behaviour, as described previously. There the predominant phase is WC for all of the milled and annealed samples with a fraction of the W_2C phase also present in the material milled for 45 h. Although the relation of the production of tungsten carbides to the milling conditions cannot be quantitatively described at present, the strong effect of ball milling on the structural evolution of milled materials has been revealed by above results. For the as-mixed starting powder, the fresh tungsten and carbon powders form W_2C when heated to 1000 °C. This W_2C phase is very stable, as shown by the phase diagram, and does not transform to WC at a temperature below 1000 °C. In the as-milled materials, things are quite different. The W_2C phase formed after milling and subsequent annealing is not stable and transforms to WC at about 900 °C. As shown in Fig. 9, extension of heat treatment at 1000 °C in vacuum to 20 h, results in the formation of material comprising almost entirely WC phase in all of the milled and annealed samples. The additional small peaks discernible in the XRD patterns are likely to be due to the Fe_3W_3C, W_6Fe_6C or other iron-containing phases resulting from the iron contamination on extended milling. Because of the relatively weak diffraction intensities, it is difficult to index them based on Fig. 9. This problem was solved by Mössbauer spectrum measurement as discussed below.

The room-temperature Mössbauer spectrum of the 310 h milled and 1000 °C 1 h annealed sample is shown in Fig. 5e. It consists of one singlet (IS ~ -0.16 mm s^{-1}) and two sextets with hyperfine magnetic fields $\sim$33 and 20.5 T, based on the normal fitting procedures. Referring to the reports on W–Fe–C [11] and Fe–C [13], the singlet represents Fe_3W_3C phase and the two sextets are α-Fe and Fe_3C. Initially we used a 50:50 at % tungsten and carbon to make up the fresh mixture. After milling and subsequent annealing, predominantly the tungsten and carbon atoms have formed WC phase. However there is also a small amount of tungsten and carbon present in the form of Fe_3W_3C. Because the ratio of tungsten and carbon in the ternary phase is 3:1, it is expected that some of the carbon will remain compared with

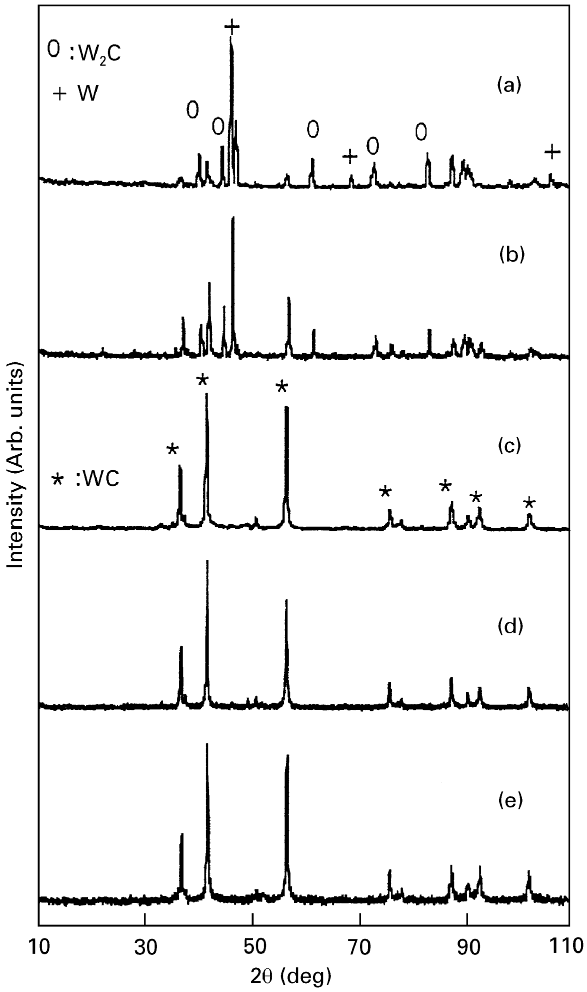

Figure 8 X-ray diffraction pattern of W50–C50 powders milled then annealed at 1000 °C for 1 h: (a) starting powder, (b) 45 h, (c) 90 h, (d) 170 h and (e) 310 h.

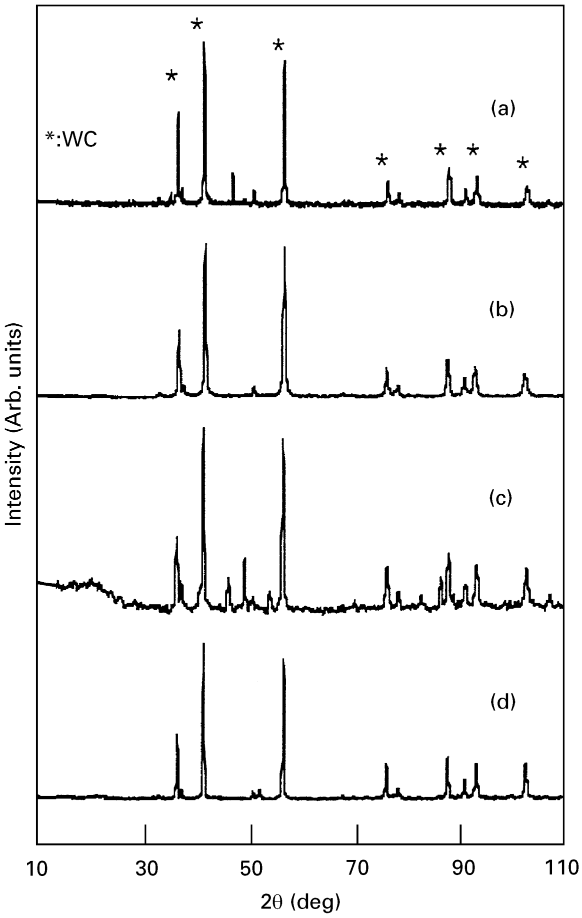

Figure 9 X-ray diffraction pattern of W50–C50 powders milled and then annealed at 1000 °C for 20 h: (a) 45 h, (b) 90 h, (c) 170 h and (d) 310 h.

tungsten. It is these carbon atoms from which the Fe_3C was formed.

4. Conclusion

Tungsten carbide, mainly WC phase, has been prepared by ball milling powder mixture of tungsten and activated carbon at room temperature. The WC phase was readily identified by X-ray and neutron diffraction following the milling of tungsten powder and activated carbon in vacuum for 170 h. Further milling to 310 h resulted in a material comprising predominantly WC in a nanostructured, disordered-like state (Fig. 1e). The propensity of the WC phase to form on ball-milling was found to be enhanced significantly on annealing the milled materials at 1000 °C in vacuum for a period of only 1 h, with samples first milled for 90 h or more being found to be comprised almost entirely of crystalline WC. The small impurity peaks discernible in the XRD patterns can, on the basis of room-temperature Mössbauer spectra, probably be identified as Fe_3W_3C phase after annealing at 1000 °C. The enhancement of the production of WC with longer milling times is reflected by the increased wear on the balls and mill, leading to increased contamination. Our continuing work on milled W–C mixtures will investigate the sintering and mechanical properties, such as hardness, of this ball mill produced WC [14].

Acknowledgements

The authors thank Ms Zhongli Li and Dr A. V. J. Edge for their help with the thermal analysis and heat treatments. The helpful discussion with Dr P. Millet is also appreciated. This work was partly supported by the Harry Triguboff AM Research Syndicate and the Australian Research Council. G.-M. Wang acknowledges receipt of a University College Postgraduate Research Scholarship.

References

1. L. E. TOTH, " Transition metal carbides and nitrides" (Academic Press, New York, 1971) p. 13.
2. R. SUNDARESAN and F. H. FROES, *J. Metals* August (1987) 22.
3. G. LE CAËR, P. MATTEAZZI, E. BAUER-GROSSE, A. PIANELLI and E. BOUZY, *J. Mater. Sci.* **25** (1990) 4726.
4. A. CALKA. J. L. NIKOLOV and B. N. NINHAM, in "Mechanical Alloying for Structural Applications", edited by J. J. De Barbadillo, F. H. Froes and R. Schwarz (ASM International, Materials Park, OH, 1993) p. 189.
5. P. MATTEAZZI and G. LE CAËR, *J. Amer. Ceram. Soc.* **76** (1991)1382.
6. A. CALKA and A. P. RADLINSKI, *Mater. Sci. Engng* **A134** (1991)1350.
7. JCPDS-ICDD No. 4-806, ICDD, Swarthmore, PA (1992) edited by R. Jenkins, W. F. McClune, M. E. Mrose, B. Post, S. Weissmann and H. F. McMurdie.
8. JCPDS-ICDD, No. 25-1047, ICDD, Swarthmore, PA (1992) edited by R. Jenkins, W. F. McClune, M. E. Mrose, B. Post, S. Weissmann and H. F. McMurdie.
9. P. M. HANSEN, "Constitution of Binary Alloys"(McGraw-Hill, New York, 1958) p. 392.
10. H. P. KLUG and L. E. ALEXANDER, "X-ray Diffraction Procedures", 2nd Edn (Wiley Interscience, New York, 1974).
11. A. CALKA, G. M. WANG and S. J. CAMPBELL, *Mater. Sci. Forum*, to be published.
12. S. J. CAMPBELL, E. WU, W. A. KACZMAREK and K. D. JAYASURIYA, *Hyper. Inter.* **92** (1994) 933.
13. G. M. WANG, A. CALKA, S. J. CAMPBELL and W. A. KACZMAREK, *Mater. Sci. Forum* **179–181** (1995) 201.
14. G. M. WANG, S. J. CAMPBELL and A. CALKA, (1995) to be published.

Received 23 February
and accepted 17 September 1996